RSC Advances

This article can be cited before page numbers have been issued, to do this please use: J. liu, J. Wang, J. Jin, F. Li, B. Li, J. Jin, C. Wang, Y. Zeng and Y. Wang, *RSC Adv.*, 2015, DOI: 10.1039/C5RA12543J.

ROYAL SOCIETY OF CHEMISTRY

www.rsc.org/advance

View Article Online
DOI: 10.1039/C5RA12543J

A combined experimental and theoretical insight into the drug delivery of nanoporous metal-organic frameworks

Jiaping Wang[a], Juncheng Jin[b], Fumei Li[a], Baohong Li[a*], Jianqiang Liu[a], Jie Jin[c], Chunfeng Wang[c], Yongping Zeng[c*], Yukun Wang[d*]

[a] *School of Pharmacy, Department of Pharmacology, and Guangdong Key Laboratory for Research and Development of Natural Drugs, Guangdong Medical University, Dongguan, 523808, P. R. China*

[b] *Technology Promotion Center of Nano Composite Material Preparation and Application; Anhui Provincial Laboratory of Biomimetic Sensor and Detecting Technology, West Anhui University, Anhui 237012, China*

[c], *College of Chemistry and Chemical Engineering, Yangzhou University, Yangzhou, 225002, China*

[d] *Department of chemistry, School of Pharmacy, Fourth Military Medical University, Xi'an, Shaanxi 710032, P. R. China*

Corresponding authors: Dr. B H. Li (gdmcli@126.com); Dr. Y. P. Zeng (*ypzeng@yzu.edu.cn*) and Y. K. Wang (wangyk@fmmu.edu.cn), Tel/Fax: 86-769-22896547

Abstract

Two isostructural nanoporous MOFs with $[Zn_3(\mu_3\text{-}O)(BTC)_2(H_3O)]_n$ (**NTU-Z11**) and $\{[Zn_3(\mu_3\text{-}O)(BTC)_2(DMF)]\cdot 2NH_2(CH_3)_2\cdot 4H_2O\}_n$ (**GDMU**) (BTC =1,3,5-benzenetricarboxylate) have been used as drug carriers of 5-fluorouracil (5-FU). The incorporation of the 5-FU into the desolvated **NTU-Z11** and **GDMU** was around 0.38 g/g and 0.22 g/g, respectively. **NTU-Z11** presents a pH-triggered controlled drug release property in 6.0, 7.4, 9.18 and water media. In addition, we performed GCMC simulations to investigate the loading of 5-FU to **NTU-Z11** and **GDMU** at the molecular level. The results from simulations reproduce the experimental trend with respect to drug loading capacity of each material. Comparison between calculated drug loading values and some molecular level properties indicates the existence of a relationship between the void space of material and drug loading capacity.

Introduction

Porous metal-organic frameworks (MOFs) have particularly highlighted for their

excellent gas-storage and catalysis properties [1-3]. Recently, tremendous efforts on MOF carriers have been made to boost their way toward medical applications [5-8]. Férey's group first described the potential loading and release properties of some drugs on MOFs[9], whereas Lin *et al*. have constructed a Pt-based drug at the nanoscale by using it as one building block to create a new coordination polymer[10]. Horcajada and his co-workers had also reported that porous MOFs can load and release drugs, acting as a promising non-toxic drug carrier [11].

Zhang and his co-worker reported a facile route to synthesize a series of **NTU**-based MOFs [12]. **NTU-Z11** is the isostructure of MOF-38 and can be repeatedly synthesized with high yield [13]; moreover, its channels are empty and have a dimension of about 11.5×11.5 Å. Inspired by these works, our strategy is to explore a neutral MOF that its structural feature is similar with **NTU-Z11**. Unfortunately, only a negative **GDMU** was obtained. But we are still interested to develop the loading and release properties of 5-FU on the two MOFs because the efficiency of drug delivery is related to the pore characteristics and the nature of host-guest interactions. GCMC simulation is a powerful technique to explain and predicate the gas adsorption to porous materials. However, there is still a challenging work to use the GCMC simulations to investigate the loading of large molecules to porous materials due to the requirement of the conformational sampling and fitting of such molecules inside tight pores [14-16].

Herein, we demonstrated two Zn(II)-based frameworks with additional negative charges that have been used as drug carriers of 5-FU. The incorporation of the 5-FU into the desolvated **NTU-Z11** and **GDMU** was around 0.38 g/g and 0.22 g/g, respectively. **NTU-Z11** presents a pH-triggered controlled drug release property in pH 6.0, 7.4, 9.18 and water media. In addition, we performed GCMC simulations to investigate the loading of 5-FU in **NTU-Z11** and **GDMU** at the molecular level. Comparison between calculated drug loading values and some molecular level properties indicates the existence of an important relationship between the void space of material and drug loading capacity.

Materials and Method

All reagents were purchased from commercial sources and used as received. IR spectra were recorded with a Perkin–Elmer Spectrum One spectrometer in the region 4000–400cm^{-1} using KBr pellets. TGA were carried out with a Metter–Toledo TA 50 under dry dinitrogen flux (60mL.min^{-1}) at a heating rate of 5°C min^{-1}. X-ray powder diffraction (PXRD) data were recorded on a Rigaku RU200 diffractometer at 60KV, 300mA for *Cu* K_α radiation (λ = 1.5406 Å), with a scan speed of 2 °C/min and a step size of 0.02° in 2θ.

X-ray Crystallography: Single crystal X-ray diffraction analyses of the two compounds were carried out on a *Bruker SMART APEX II CCD*diffractometer equipped with a graphite monochromated Mo*K*α radiation (*λ* = 0.71073 Å) by using *ϕ*/*ψ* scan technique at room temperature. The intensities were corrected for Lorentz and polarization effects as well as for empirical absorption based on multi-scan techniques; all structures were solved by direct methods and refined by full-matrix least-squares fitting on F^2 by SHELX-97[17]. Absorption corrections were applied by using multi-scan program SADABS[18]. Non-hydrogen atoms were refined anisotropically. The structure contains large (37 % volume) regions of intensely disordered cations and solvent. These were impossible to model at atomic resolution and their presence in the structure is assumed on the basis of the elemental analysis, TGA and the PLATON/SQUEEZE calculations [19]. The latter were used to calculate the diffraction contribution of the solvent molecules and, thereby, to produce a set of solvent-free diffraction intensities for the refinement of the MOF structure. Crystallographic data for complexes **GDMU** are given in Table 1. Selected bond distances and bond angles are listed in Table 2. **CCDC**: 1405443 for **GDMU**.

Syntheses of these complexes

$[Zn_3(\mu_3\text{-}O)(BTC)_2(H_3O)]_n$ (**NTU-Z11**)

We only synthesized the **NTU-Z11** according to the reference. The sample purity was confirmed by the PXRD.

$\{[Zn_3(\mu_3\text{-}O)(BTC)_2(DMF)]\cdot 2NH_2(CH_3)_2\cdot 4H_2O\}_n$ (**GDMU**)

A mixture of $Zn(NO_3)_2\cdot 6H_2O$ (0.450g, 0.1mmol), L(4,4'-bis(pyrid-4-yl)biphenyl) (0.015g, 0.04mmol), and H_3BTC (0.450mg, 0.2mmol), DMF (4mL) in a

screw-capped vial. After five drops of HNO_3 was added into the mixture. The vial was capped and placed in an oven at 110 ºC for 3 days. The resulting colorless single crystals were washed with absolute CH_3CH_2OH three times to give **1**. Anal. Calcd for $C_{25}H_{37}N_3O_{18}Zn_3$ (863.68), C, 34.77; H, 4.32; N, 4.87. Found C, 34.28.; H, 4.15; N,4.55. IR (KBr, cm^{-1}) : 3480(vs); 2940(m); 1632(vs); 1428(v); 1390(v); 1099(m); 938(m); 708(v); 547(m).

Computational Details

The 5-FU adsorption in **NTU-11** and **GDMU** was studied using grand canonical ensemble Monte Carlo (GCMC) simulations, employed with the RASPA code at 298 K[20]. The structures of 5-FU and MOFs are described with an all-atom model in this work. The structures for 5-FU and MOFs can be found in Figures S1 and S2. For MOFs structures, the framework atoms were kept rigid during the simulations. The guest-guest and guest-host interactions were computed with a Lennard-Jones (LJ) and Coulombic potential. The Antechamber program of AmberTools1.27 was used to generate the force field for 5-FU with the general amber force field parameters [21]. The atomic partial charges for 5-FU were computed with CHELPG method based on the Gaussian 03 suite with the 6-31++g* basis set. The Lennard-Jones parameters and partial charges can be found in Table S1- S3.

The atomic positions of **NTU-Z11** and **GDMU** structures were taken from the PXRD data(The Rietveld refinement for the 5-FU@MOFs complexes was performed with the software GSAS/EXPGUI, using the X-ray structure of the MOF as initial atomic coordinates.). The cations of H_3O^+ and $NH_2(CH_3)_2^+$ are included in **NTU-Z11** and in **GDMU**, respectively. The cations of $NH_2(CH_3)_2^+$ were not removed in the uptake of 5-FU. Thus we also did not remove these molecules in these simulated structures. The Lennard-Jones parameters for the MOFs structure atoms were taken from the UFF force field (listed in Table S2) [22]. The accurate prediction of adsorption in various MOFs could be achieved by a number of simulation investigations using the UFF force field [23-24]. The molecular geometries for cations were optimized by DFT method. In canonical ensemble, the desired number of cation were inserted into the pore and attempted to accelerate the equilibrium with

reinsertion-move. The obtained configurations were used to simulate the adsorption of 5-FU in MOFs. The solvent molecules of the MOFs in the simulations are allowed to move (including translation and rotation).

The heats of adsorption were computed using the equation:

$$Q_{st} = RT - \frac{\langle UN \rangle - \langle U \rangle \langle N \rangle}{\langle N^2 \rangle - \langle N \rangle^2}$$

where < > refers to the average over the simulation, and U is the energy, N is the number of adsorbed molecules.

For the interactions of unlike sites were computed with Lorentz-Berthelot mixing rules. The Lennard-Jones interactions were cut and shifted at the 13 Å. The partial charges of the **NTU-Z11** and **GDMU** atoms were computed from density functional theory (DFT) with the B3LYP functional. For the metal atoms, the LanL2DZ basis set was applied. The 6-31++g* basis set was used to optimized for all other atoms. The atomic partial charges can be obtained by fitting the electrostatic potentials after DFT computation. The Coulombic interactions were computed using the Ewald sum technique. The details of simulated boxes are listed in Table S4. After the initial 10^6 Monte Carlo (MC) cycles, the production of 10^6 cycles was used to compute the ensemble averages properties. For each cycle, the MC moves include the molecule of insertion, deletion, translation, rotation or re-growth. We used the equal probability for each MC moves.

Results and Discussion

$[Zn_3(\mu_3\text{-}O)(BTC)_2(H_3O)]_n$ (**NTU-Z11**) and $\{[Zn_3(\mu_3\text{-}O)(BTC)_2(DMF)]\cdot 2NH_2(CH_3)_2\cdot 4H_2O\}_n$ (**GDMU**)

The **NTU-Z11** and **GDMU** are isostructural, which are composed of the $[Zn_3(\mu_3\text{-}O)(COO)_6]$ subunits (Fig. 1a-1b). The subunits are connected by BTC ligands, which results in an infinite 3-D (3,6)- connected framework with 1-D channel of about 11.5 × 11.5 Å dimension along the *c*-axis (Figure 1c-1d). But we should state herein, if the L was absent in this reactive system, the final product of **GDMU** could not be obtained. Furthermore, the pores of **GDMU** were occupied by the $NH_2(CH_3)_2$

and DMF molecules. This structural feature was also similar with MOF-38, which holds some disordered HTEA molecules. However, the MOF-38 cannot be repeated as mentioned in the literature[13].

Thermogravimetric Analyses

The thermogravimetric analyses (TGA) of complex **GDMU** was performed (Fig. S3). It shows three weight loss steps. The first weight loss begins at 25°C and is completed at 80°C. The observed weight loss of 8.6% is corresponding to the loss of the free water molecules (calcd 8.3%). The second weight loss occurs latterly, and can be attributed to the elimination of $NH_2(CH_3)_2$ cations(obsd: 9.5%; calcd 10.4%). A gradual weight loss from 210 °C indicates that the complex decomposes continuously when the temperature is raised. The mass remnant at ~700 °C of 25.4 % is roughly consistent with the deposition of ZnO (calcd 28.3%) (a weight loss of 4.0% is larger than the calculated value, probably resulting from the sensitivity to temperature and humidity or a very slow absorbability of the guest molecules from the air at room temperature).

Both of **NTU-Z11** and **GDMU** were desolvated at 120 °C for 10 h prior to insertion of the drug. As confirmed by PXRD and TGA, 5-FU containing sample maintains its crystallinity (Fig. S3 and Fig. S4), thus, the drug encapsulation did not alter the structure of these materials. Only a decrease in the intensity of the low angle reflections on the PXRD patterns (~5-8° 2θ) was observed after encapsulation, following the change in pore content that is known to strongly affect the relative intensities of the Bragg peaks[2b]. This was confirmed by N_2 adsorption analyses showing that the BET surface area significantly decease upon drug molecules loading (see Supplementary Information Fig. S5).

Incorporation of the drug molecule during loading process has been recorded by Fourier transformed infrared spectroscopy (FTIR) (Figure S6). The absorption bands of C–F deformations were discovered in the 820–550 cm^{-1} regions. The absorption band at about 1240 cm^{-1} may be due to fluorine atom on the ring [25-26]. Based on the above structural analyses, these two compounds may be taken as a good drug carrier. The loading of anticancer 5-FU was carried out by impregnating **NTU-Z11**

and **GDMU** under stirring in 5-FU containing ethanol solutions.

UV–vis absorption spectroscopy has been used to determine the effective storage capacity, To reach a maximal drug loading, 5-FU to porous solid relative ratio and contact time were evaluated (Table S5)[6]. The loading amount of 5-FU increased with initial 5-FU/material ratio repressed in weight and optimal value 1:1 and 1:3 for **NTU-Z11** and **GDMU** in ethanol, respectively. The contact time was also important, the maximum adsorption was obtained after 2 days and 3 days for **NTU-Z11** and **GDMU**, respectively. Thus, the best results were obtained when **NTU-Z11** was soaked for 2 days within a 5-FU to material weight ratio of 1:1, while **GDMU** was soaked for 3 days within a 5-FU to material weight ratio of 1:3. 5-FU was incorporated into desolvated **NTU-Z11** and **GDMU** with loadings of 0.382 and 0.206 g/g, respectively. The difference between **NTU-Z11** and **GDMU** shows that the $NH_2(CH_3)_2$ takes as gate and blocks the drug molecules access to inner pores [27].

Fig. 2 shows the release profile of the drug delivery system of **NTU-Z11** and **GDMU** in PBS solution at 37 ℃. At the first stage (24 hours), the **NTU-Z11** and **GDMU** have the similar releasing behavior and approximately 65 % of the drug was released. However, the other part released gradually in **GDMU**, implying a strong host-guest interaction involved in this process. Compared with the **NTU-Z11** carrier, there is a big cation in the host channels in **GDMU**, which can take as donor/acceptor and bind to drug molecules resulting in the dramatically releasing behavior. Thus, 5-FU with flat molecular shape diffuses along the hexagonal channels. Similar results were also found in MIL-53 with a pore size of 8.6 Å exhibited a drug loading capacity of 0.22 g/g for drug IBU (IBU = ibuprofen) [3].

To further explore the pH-responsive drug release feature of **NTU-Z11**, release profile were performed in pH 6.0, 9.18 and water medium. Around 62.5% of the loaded 5-FU was released fast within 24 h, and 63.1% within 30 h. More than 40% of 5-FU released around one hour, which consistent with dissolution of **NTU-Z11** in acidic environment. Compared with other MOF carriers[28], **NTU-Z11** shows a fast release rate for 5-FU. In the water medium, the released profile of 5-FU exhibits a flat shape and occurs no burst effect. The delivery of 5-FU occurred within 96 h and 47 %

of the loaded drug was released. However, three stages related to the drug release could be distinguished in pH 9.18, around 48% of the loaded drug was released in the first stage (33 h) and only almost not more than 10% of the loaded drug was released. Thus, a rapid releasing process was observed during the first stage followed by a slower in the high pH. These results imply that the loaded drug can be decreased during blood circulation and the drug release rate is suddenly accelerated after release into cancer cells [25, 29].

Computational Simulations of 5-FU Adsorption

The amount of drug per porous material or drug loading is one of the main quantities of interest in the use of MOFs for controlled drug release [30]. We have used GCMC simulations to investigate the loading of 5-FU to two compounds at the molecular level. These simulations were used to determine the preferential binding sites of the 5-FU in the porous materials, to estimate the maximum drug loading capacity of each material, and propose a molecular mechanism for drug loading and release.

Adsorption isotherm of 5-FU in MOFs

We calculated the adsorption isotherms of 5-FU in **NTU-Z11** and **GDMU** 298 K. As observed in Figure 3, there are some differences between **NTU-Z11** and **GDMU**. The **NTU-Z11** has much higher saturation capacity for 5-FU, which is about 0.4 g/g. The saturation capacity is around 0.22 g/g for **GDMU**. The bigger molecules of **GDMU** result in a low saturation capacity compared to that of **NTU-Z11**. Also, **GDMU** show a saturation uptake at the low fugacity range due to the stronger 5-FU-MOF interactions. The presence of stronger interaction due to the existence of cations in **GDMU** strengthens the host-guest interactions and results in the steep adsorption of 5-FU at lower fugacity than in **NTU-Z11**.

Heat of adsorption

The heats of adsorption (Q_{st}) for 5-FU in **NTU-Z11** and **GDMU** studied are shown in Fig. 4. The heat of adsorption is closely related with the pore structure, in which could be taken as an index of the adsorption materials heterogeneity [30]. Fig. 4

shows the Q_{st} for **NTU-Z11** and **GDMU** as the function of uptake. As observed in Fig.4, the **NTU-Z11** shows the low Q_{st} (about 120-150 kJ/mol) at the loadings process. This observation shows that the 5-FU molecules can load into MOFs pores with strong interaction. The stronger interaction results in the higher adsorption heat of 5-FU than in NTU-Z11 because of the presence of DMF in GDMU. The **GDMU** shows the higher Q_{st} (160-228 kJ/mol) at the range of loadings. The medicine molecules can be strongly retained in the MOF structures due to the high Q_{st} at the loadings and it is very favorable for the long release process. **GDMU** shows higher Q_{st} values than **NTU-Z11** at high loadings, with the important contributions of the solvent molecules. The results are consistent with experimental released process.

Density plots

NTU-Z11 consists of the trimetric SBU and BTC ligand. The 3-D framework has two channel systems with dimension of 7.5 × 7.5 Å (refer to as A) and 11.5 × 11.5 Å (refer to as B) along the *c*-axis. As observed in Fig. 5, the 5-FU molecules are primarily distributed in the two favorable regions. The 5-FU loading is closely packed in the pores because the solvent molecules have a smaller size in A region. The bigger cations present in **GDMU** hinder the adsorption of 5-FU in A region. Then the adsorption of 5-FU in **NTU-Z11** increases with the increase of fugacity. However, the adsorption of 5-FU in **GDMU** rapidly approaches to a platform at same range of pressure.

Conclusion

In summary, two isostructural nanoporous MOFs were used to load anti-cancer chemotherapy drug 5-FU and demonstrated a remarkable different capacity due to their various pore spaces. Owing to pH-sensitive property of **NTU-Z11**, it was observed that it released much faster in mild acidic buffer solution than at a neutral medium, suggesting that this pH-triggered feature may be useful property for drug delivery to tumors. GCMC simulations suggested that the anti-cancer drug 5-FU could load to the **NTU-Z11** in high loading capacity. Our findings indicate that the combined experimental-computational approach is a powerful strategy for the efficient identification and incorporation of bioactive compounds in porous materials.

Acknowledgments

This work was partially supported by the grants from the National Natural Science Foundation of China (21201044, 21401143 and 20806064), Science and Technology Project of Anhui Province (Grants 1206c0805031 and 1406c085021), Shaanxi Province science and technology key projects (2011K12-03-01). Y. Z. acknowledges funding from the Natural Science Foundation of Jiangsu Province, China (BK20131227).Generous allocations of computer time were provided by the ScGrid plan of Supercomputing center of CAS and Testing Center of Yangzhou University and a Project funded by the Priority Academic Program Development of Jiangsu Higher Education Institutions and thanks for Prof. S. W. Ng for refinement of structural data.

References:

[1] Q. Zhai, Q. Lin, T. Wu, L. Wang, S. Zheng, X. Bu and P. Feng, Chem. Mater., 2012, **24**, 2624;
(b) Y. J. Cui, Y. F. Yue, G. D. Qian and B. L. Chen, Chem. Rev., 2012, **112**, 1126;
[2] J.-P. Zhang, Y.-B. Zhang, J.-B. Lin and X.-M. Chen, Chem. Rev., 2012, **112**, 1001.
[3] G. Férey, C. Mellot-Draznieks, C. Serre and F. Millange, *Acc.Chem. Res.* 2005, ***38***, 217.
[4] C. Wu and W. Lin, *Angew. Chem. Int. Ed.* 2007, ***46,*** 1075.
[5] J. Zhuang, C. H. Kuo, L. Y. Chou, D. Y. Liu, E. Weerapana and C. K. Tsung, ACS. Nano., 2014, **8**, 2812.
[6] P. Horcajada, C. Serre, G. Maurin, N. A. Ramsahye, F. Balas, M. Vallet-Regi, M. Sebban, F. Taulelle and G. Ferey, J. Am. Chem. Soc. 2008, **130**,6774.
[7] G. Férey , *Chem. Soc. Rev.* 2008 , ***37*** , 191
[8] K. M. L. Taylor , A. Jin and W. B. Lin , *Angew. Chem.* 2008 , ***120*** , 7836
[9] P. Horcajada , C. Serre , M. Vallet-Regi , M. Sebban , F. Taulelle and G. Férey , *Angew. Chem.* 2006 , ***118*** , 6120
[10] K. M. L. Taylor-Pashow, J. D. Rocca, Z. G. Xie, S. Tran and W. B. Lin, J. Am. Chem. Soc., 2009, **131**, 14261.
[11] P. Horcajada, T. Chalati, C. Serre, B. Gillet, C. Sebrie, T. Baati, J. F. Eubank, D. Heurtaux, P. Clayette, C. Kreuz, J. S. Chang, Y. K. Hwang, V. Marsaud, P. N. Bories, L. Cynober, S. Gil, G. Ferey, P. Couvreur and R. Gref, Nature Mat. 2010, **9**, 172.
[12] J. K. Gao, K. Q. Ye, L. Yang, W. W. Xiong, L. Ye, W. Wang and Q. C. Zhang, Inorg. Chem., 2014, **53**, 691.
[13] J. Kim, B. Chen, T. M. Reineke, H. Li, M. Eddaoudi, D. B. Moler, M. O'Keeffe and O. M. Yaghi, J. Am. Chem. Soc. 2001, **123**, 8239.
[14] T. Düren, L. Sarkisov, O. M. Yaghi and R. Q. Snurr, *Langmuir.* 2004, ***20,*** 2683.
[15] Q. Yang, C. Zhong and J. F. Chen, *J. Phys. Chem. C.,* 2008, ***112*** , 1562.
[16] T. Düren, Y. S. Bae and R. Q. Snurr, *Chem. Soc. Rev.* 2009, ***38***, 123.
[17] G.M. Sheldrick, Acta Cryst. 2008, **A64**, 112.
[18] G. M. Sheldrick, Bruker AXS, SAINT Software reference Manual, Madison, WI, 1998
[19] A. L. Spek, J. Appl. Crystallogr. 2015, **C71**, 9.
[20] D. Dubbeldam, S. Calero, D. E. Ellis and R.Q Snurr, *Mol. Simulat.* 2015, ***1***, 1
[21] D. A. Case, T. A. Darden, III, T. E. Cheatham, C. L. Simmerling, J. Wang, R. E. Duke, R. Luo, R.

C. Walker, W. Zhang, K. M. Merz, B. Roberts, B. Wang, S. Hayik, A. Roitberg, G. Seabra, I. Kolossvai, K. F. Wong, F. Paesani, J. Vanicek, J. Liu, X.Wu, S. R. Brozell, T. Steinbrecher, H. Gohlke, Q. Cai, X. Ye, J.Wang,M. J. Hsieh, G. Cui, D. R. Roe, D. H. Mathews, M. G. Seetin, C. Sagui, V. Babin, T. Luchko, S. Gusarov, A. Kovalenko and P. A. Kollman, AMBER 11, University of California, San Francisco, 2010.

[22] A. K. Rappe, C. J. Casewit, K. S. Colwell, W. A. Goddard III and W. M. Skiff, J. Am. Chem. Soc., 1992, **114**, 10024.

[23] K. M. Gupta, Y. Chen and J. Jiang, J. Phys. Chem. C, 2013, **117**, 5792.

[24] C. E. Wilmer, K. C. Kim and R. Q. Snurr, J. Phys. Chem. Lett., 2012, **3**, 2506.

[25] C. Y. Sun, C. Qin, X. L. Wang, G. S. Yang, K. Z. Shao, Y. Q. Lan, Z. M. Su, P. Huang, C. G. Wang and E. B. Wang, Dalton Trans., 2012, **41,** 6906.

[26] C. Y. Sun, C. Qin, C. G. Wang, Z. M. Su, S. Wang, X. L. Wang, G. S. Yang, K. Z. Shao, Y. Q. Lan and E. B. Wang, Adv. Mater, 2011, **23**, 5629.

[27] S. T. Meek, J. A. Greathouse, M. D. Allendorf, Adv. Mater., 2011, **23**, 249.

[28] P. Horcajada, C. Serre, M. Vallet-Regi, M. Sebban, F. Taulelle and G. Ferey,Agnew. Chem. Int. Ed., 2006, **45**, 5974.

[29] S. F. Yan, J. Zhou, Z. C. Wang, J. B. Yin, Y. Z. Zheng and X. S. Chen. Eur. J. Pharm. Biopharm., 2011, **78**, 336.

[30] M. C. Bernini, D. Fairen-Jimenez, M. Pasinetti, A. J. Ramirez-Pastor and R. Q. Snurr, *J. Mater. Chem. B,* 2014, ***2*****,** 766.

View Article Online
DOI: 10.1039/C5RA12543J

Main Figures and Tables

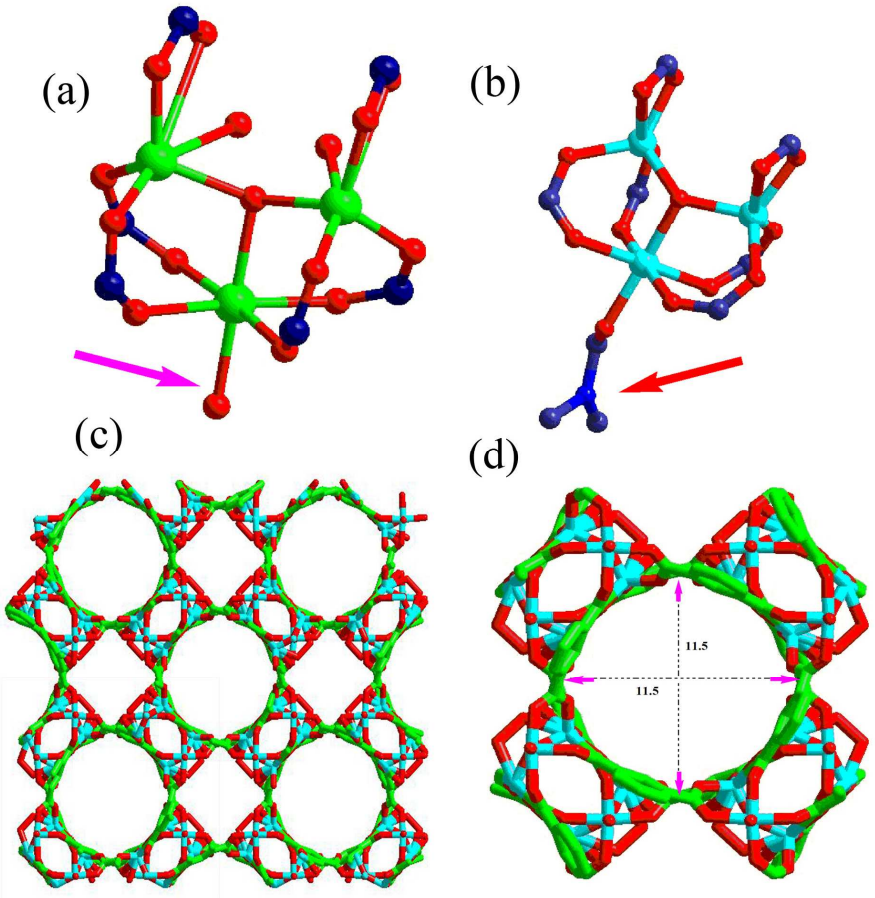

Fig. 1 (a) the geometries of metal and ligands in NTU-Z11; (b) view of the geometries of the metal and ligands in **GDMU**; (c) view of the 3D frameworks and (c) the larger hexagonal channel in the MOFs.

View Article Online
DOI: 10.1039/C5RA12543J

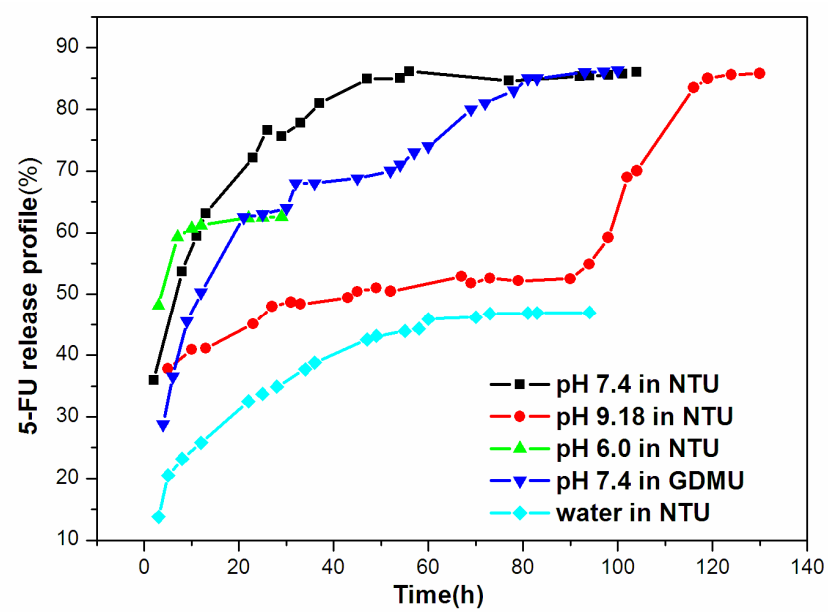

Fig.2 5-FU delivery (% 5-FU *vs. t*) from NTU and **GDMU** and schematic illustration shows the 5-FU load and release process.

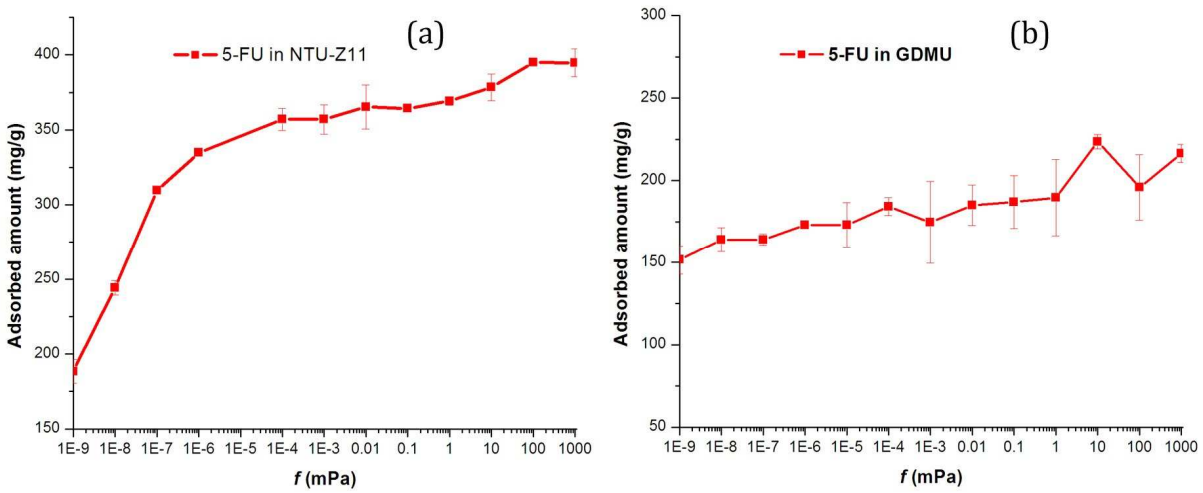

Fig. 3 (a) and (b) the calculated adsorption isotherm of 5-FU in **NTU-Z11** and **GDMU** at 298K, respectively.

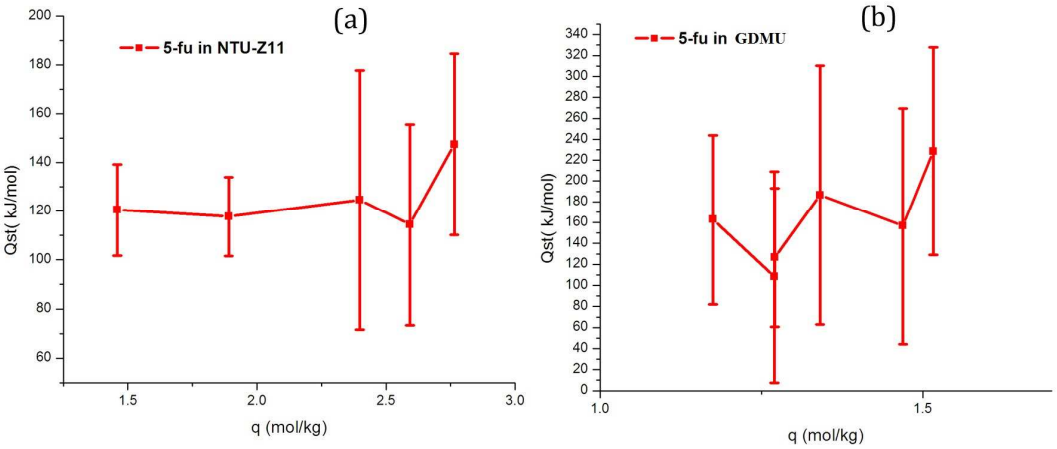

Fig. 4 (a) and (b) the calculated heats of adsorption of 5-FU in **NTU-Z11** and **GDMU** at 298K, respectively.

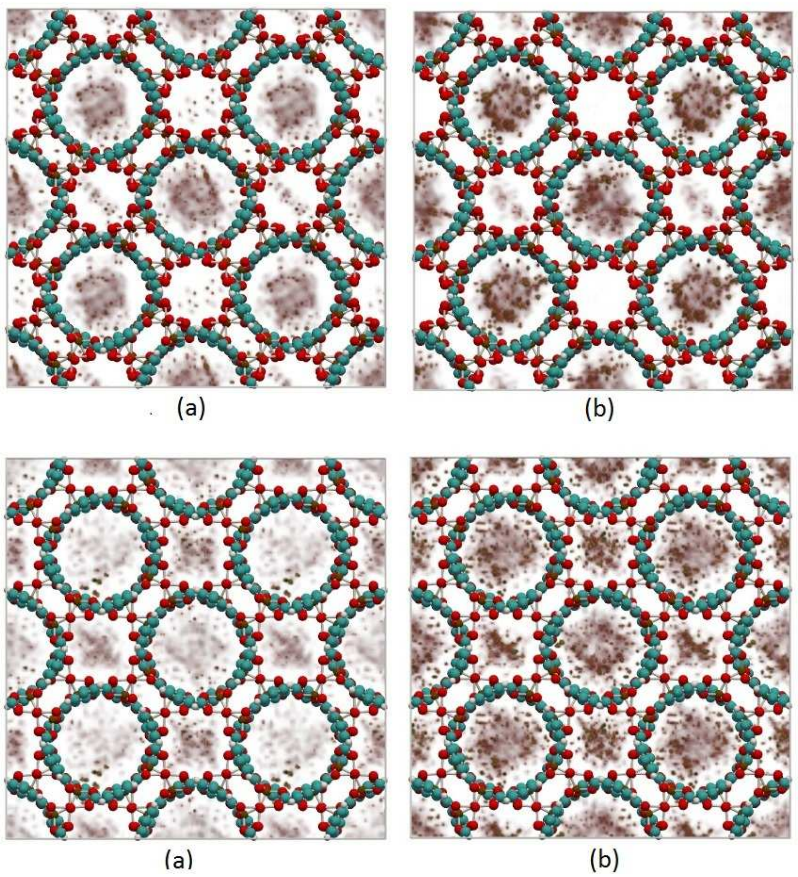

Fig. 5 The density of 5-FU in **GDMU** at 298 K (a) 10^{-9} mPa (b) 10^{-7} mPa (above) and The density of 5-FU in **NTU-Z11** at 298 K (a) 10^{-9} mPa (b) 10^{-7} mPa (below).

View Article Online
DOI: 10.1039/C5RA12543J

Table 1. Crystal data and structure refinement information for compound **GDMU**

Crystal system	tetragonal
Space group	*I 4 c m*
Crystal color	Colorless
a, Å	20.5138(10)
c, Å	17.8100(8)
γ	90
V, Å ^{3}	7494.7(8)
Z	8
ρ_{calcd}, g/cm^3	1.531
F(000)	3536
θ Range, deg	2.49-27.92
Reflns collected/unique(Rint)	21512/ 4425 (0.0299)
GOF	1.092
R_1, wR_2 ($I > 2\sigma(I)$)*	0.0319, 0.0900
R_1, wR_2 (all data)**	0.0357, 0.0924

* $R = \sum(F_o - F_c)/\sum(F_o)$, ** $wR_2 = \{\sum[w(F_o^2 - F_c^2)^2]/\sum(F_o^2)^2\}^{1/2}$.

Table 2. Selected bond distances (Å) and angles (deg) of structure **GDMU**

Zn1-O1	1.945(4)	Zn1- O8	1.9458(17)
Zn1- O4	1.969(3)	Zn1- O5	1.972(3)
Zn2- O7	2.059(5)	Zn2- O3	2.091(3)
Zn2- O3	2.091(3)	Zn2- O8	2.103(4)
Zn2- O6	2.106(3)	Zn2- O6	2.106(3)
O1- Zn1 -O8	113.76(18)	O1- Zn1- O4	123.14(16)
O8- Zn1- O4	105.27(16)	O1- Zn1- O5	103.53(16)
O8 -Zn1- O5	103.27(17)	O4- Zn1- O5	105.86(18)

1	O7 -Zn2- O3	86.24(14)	O3- Zn2- O3	97.10(17)
2	O7- Zn2 -O8	171.1(2)	O3 -Zn2 -O8	87.85(12)
3	O3- Zn2 -O8	87.85(12)	O7- Zn2- O6	91.29(15)
4	O3 -Zn2- O6	173.17(14)	O3- Zn2- O6	89.08(15)
5				